BIOCHEMICAL PHARMACOLOGY 74 (2007) 679–689

available at www.sciencedirect.com

ScienceDirect

journal homepage: www.elsevier.com/locate/biochempharm

Mechanism of acridine-based telomerase inhibition and telomere shortening

Mekala Gunaratnam [a], *Olga Greciano* [a], *Cristina Martins* [a], *Anthony P. Reszka* [a], *Christoph M. Schultes* [a], *Hamid Morjani* [b], *Jean-Francois Riou* [b], *Stephen Neidle* [a,*]

[a] *CRUK Biomolecular Structure Group, The School of Pharmacy, University of London, 29-39 Brunswick Square, London WC1N 1AX, UK*
[b] *Laboratoire d'Onco-Pharmacologie, JE 2428, UFR de Pharmacie, Universite de Reims Champagne-Ardenne, 51 Rue Cognacq-Jay, F 51096 Reims, France*

ARTICLE INFO

Article history:
Received 14 May 2007
Accepted 5 June 2007

Keywords:
G-quadruplex ligands
Telomerase
Telomere targeting

ABSTRACT

The trisubstituted acridine compound BRACO-19 has been developed as a ligand for stabilising G-quadruplex structures. It is shown here that BRACO-19 produces short- and long-term growth arrest in cancer cell lines, and is significantly less potent in a normal cell line. BRACO-19 reduces telomerase activity and long-term telomere length attrition is observed. It is also shown that BRACO-19 binds to telomeric single-stranded overhang DNA, consistent with quadruplex formation, and the single-stranded protein hPOT1 has been shown to be displaced from the overhang *in vitro* and in cellular experiments. It is concluded that the cellular activity of BRACO-19 can be ascribed both to the uncapping of 3′ telomere ends and to telomere shortening that may preferentially affect cells with short telomeres.

1. Introduction

Telomeres are specialised nucleoproteins that protect the end of chromosomes from recombination, degradation and end-to-end fusions [1]. Telomeres in somatic cells progressively shorten with each successive round of cell division until they reach a critical length, at which point cells cease to divide and enter the non-replicative and irreversible state of senescence. In somatic cells, telomeres can range from 15 to >20 kb in length. By contrast, telomeres are significantly shorter and are maintained at a constant length in cancer cells [2,3], in most cancer cell types by telomerase, a ribonucleoprotein complex [4,5], allowing indefinite proliferative potential. The catalytic subunit of this enzyme, hTERT, adds repeats of TTAGGG to the ends of human chromosomes using a template on a separate RNA domain (hTR). While telomerase is not an oncogene, transfection of hTERT into normal epithelial or endothelial cells with SV40 antigen and N-ras oncogene permits cells to bypass senescence and acquire tumorigenicity, supporting its pivotal role in cancer development [6,7]. A number of studies have demonstrated that inhibition of telomerase in cancer cells leads to senescence and apoptosis [8–11]. One approach to achieve this targets the telomerase RNA template directly with oligonucleotides that inhibit recognition of the extreme 3′-end nucleotides of the telomere, the initial step in telomerase processing; an oligonucleotide to achieve this, GRN163L, is currently in clinical trial [12]. Clinical trials with vaccines using antigenic peptides against telomerase are also underway [13].

In vertebrates, telomeres consist of tandem repeats of guanine (G) rich duplex DNA sequences of 5′-TTAGGG-3′, where the 3′-end extends to form a single-stranded overhang of 150–250 nt [14–16]. This overhang can form a higher-order DNA G-quadruplex structure under appropriate conditions,

* *Corresponding author*. Tel.: +44 207 753 5969; fax: +44 207 753 5970.
E-mail address: stephen.neidle@pharmacy.ac.uk (S. Neidle).
0006-2952/$ – see front matter
doi:10.1016/j.bcp.2007.06.011

although in cellular conditions binding of the single-strand binding protein hPOT1 normally inhibits quadruplex formation [17]. Formation of intramolecular quadruplex structures halts the synthesis of further telomeric DNA repeats since the 3′-end can no longer be recognised by the hTR RNA template of the telomerase complex [18,19]. Quadruplex formation can be induced by appropriate quadruplex-binding ligands, which thus indirectly inhibit telomerase function [20]. A large number of such ligands have been subsequently reported, mostly based on a core of a polycyclic aromatic system together with cationic side-chains that stabilise G-quadruplex structures [21–24]. There is extensive data on the interactions of these compounds with G-quadruplexes [25–37], and a rapidly-growing number of reports of their cellular behaviour [38–46]. Their effects as Telomere Targeting Agents (TTAs), hindering telomere elongation and maintenance, lead to telomere shortening, senescence and cell death. TTAs are thus currently being explored as a new type of molecularly targeted anticancer agent.

Our goal is the development of the TTA concept into clinically-useable agents. To that end we designed a series of 3,6,9 trisubstituted acridine-based TTA molecules using structure-based drug design [47], and have developed structure–activity relationships for derivatives with a wide range of substituents [48,49]. A lead compound, BRACO-19 (Fig. 1), has been previously shown to produce cell growth arrest, end-to-end chromosomal fusions [50], and anticancer activity in tumour xenografts [51,52]. We report here on a mechanistic study of the cellular effects of BRACO-19, using a series of short- and long-term growth inhibition studies in a range of human cancer cell lines to probe the underlying mechanisms of action of BRACO-19.

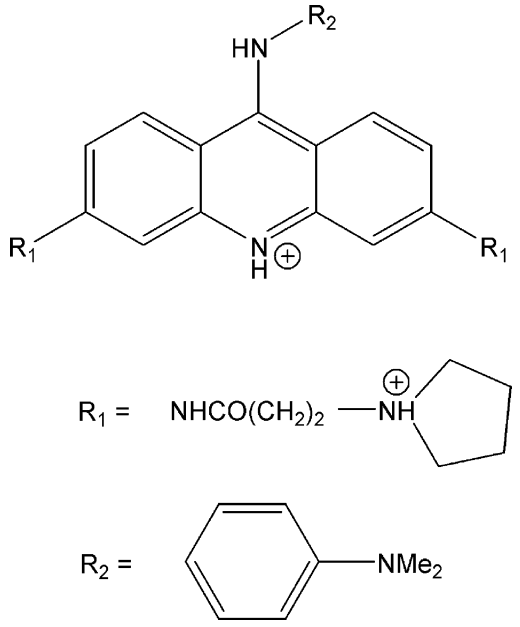

Fig. 1 – Structure of BRACO-19 as the salt, showing sites of protonation under physiological conditions.

2. Materials and methods

2.1. *Preparation of compounds*

The TTA compound BRACO-19 was synthesized in-house using previously published procedures [47–49], and was judged to be analytically pure as the free base and kept at −20 °C. 10 mM stock solutions were prepared in dimethylsulphoxide (DMSO, Sigma) and kept at 4 °C. On the day of an experiment, stock solutions were diluted to a 1 mM working concentration in filtered sterilized deionised water and 1% HCl.

2.2. *Cell lines*

Human cancer cell lines, breast (MCF7), lung (A549), ovarian (A2780), prostate (DU145), colon (HT-29), HGC-27 (gastric) and A2780 (ovarian) and two normal human lung fibroblast lines (IMR90 and WI-38) were purchased from American Type Cell Culture (ATCC). All cell lines except HGC27 and WI38 were maintained in Dulbecco's Modified Eagles Media containing 10% foetal bovine serum (Invitrogen, UK), 0.5 μg/ml hydrocortisone (Acros Chemicals, Loughborough, UK), 2 mM L-glutamine (Invitrogen, Netherlands), and non-essential amino acids 1× (Invitrogen, Netherlands), and incubated at 37 °C, 5% CO_2. MCF7, A549 and IMR90 cell lines were routinely passaged at 1:6 and DU145 and A2780 at 1:20 twice a week. The WI38 and HGC27 lines were maintained in minimum essential medium, prepared as above.

The sulphorhodamine B (SRB) short-term cytotoxicity assay was performed on all cell lines. Long-term growth inhibition studies were also carried out on MCF7, A549 and DU145 cell lines. MCF7 and A549 cells lines were used for studies of senescence and apoptosis induction, and the former was used for subsequent detailed mode of action studies.

2.3. *Sulphorhodamine B short-term cytotoxicity assay*

Short-term growth inhibition was measured using the SRB assay as described previously [49]. Briefly, cells were seeded (4000 cells/wells) into the wells of 96 well-plates in DMEM and incubated overnight as before to allow the cells to attach. Subsequently cells were exposed to freshly-made solutions of BRACO-19 at increasing concentrations of 0, 0.1, 1, 5 and 25 μM in quadruplicate and incubated for a further 96 h. Following this the cells were fixed with ice cold trichloaceticacid (TCA) (10%, w/v) for 30 min and stained with 0.4% SRB dissolved in 1% acetic acid for 15 min. All incubations were carried out at room temperature. The IC_{50} value, concentration required to inhibit cell growth by 50%, was determined from the mean absorbance at 540 nm for each drug concentration expressed as a percentage of the control untreated well absorbance.

2.4. *Telomerase repeat amplification protocol*

Inhibition of telomerase activity following long-term exposure to BRACO19 was measured using the telomerase repeat amplification protocol (TRAP) assay. Protein (500 ng) from MCF7 cells treated for 2 weeks with BRACO19 was incubated with TS primer (0.1 μg, 5′-AATCCG TCG AGC AGA GTT-3′) at 30 °C for 10 min to enable elongation of primer by telomerase.

Following this the elongated products were amplified using ACX primer (1 μM, 5′-GCG CGG [CTTACC]$_3$ CTA ACC-3′) at 92 °C (33 cycles of 92 °C for 30 s, 55 °C for 30 s, 72 °C for 45 s). Both TS and ACX primers were purchased from Invitrogen. The PCR products were resolved on a 10% polyacrylamide gels, stained with SYBR green (Sigma) and quantified using gel scanner and gene tool software (Sygene, Cambridge, UK). The EC_{50} values, concentration of ligand required to inhibit 50% of telomerase activity was calculated.

2.5. Long-term growth inhibition studies

1×10^5 cells were seeded in 75 cm^2 tissue culture flasks and exposed to sub-cytotoxic concentrations of BRACO-19. The concentrations were chosen according to individual IC_{50} values as determined in the SRB assay. Cells were grown in a final volume of 10 ml DMEM and incubated as described previously. Cells were exposed to BRACO-19 twice a week by replacing with fresh media containing drug on day 3. On day 7 media was removed and cells were washed with PBS once and trypsinised using 3 ml of trypsin. Cells were then pelleted and resuspended in 10 ml of DMEM and viability was determined with a haemocytometer. From this 1×10^5 cells were reseeded and experiment was continued as described before. The remaining cells were centrifuged and stored at −80 °C for further analysis.

2.6. Effects on DNA, RNA and protein synthesis

The effects of BRACO-19 on DNA, RNA and protein synthesis were measured by 24 h labelling of cells with either ^{3}H-thymidine, ^{3}H-uridine or ^{3}H-leucine, respectively. [Methyl-^{3}H] thymidine (3.03 Tbq/mmol), [5,6-^{3}H] uridine (1.6 TBq/mmol) and L-[4,5-^{3}H] leucine (5.62 TBq/mmol) were purchased from Amersham Biosciences. Cells were seeded at a density of 10^5 cells/cm^2 in 25 cm^2 flask in 5 ml DMEM and incubated overnight. Following this the medium was removed and replaced with medium containing 0, 1, 2, 5, 7.5 and10 μM BRACO-19 and 37 KBq (1 μCi) of tritiated precursor and incubated for further 4 h. For each treatment and precursor, experiments were set up in quadruplicates. At the end of incubation, one flask from each treatment point was taken and trypsinised as described before and viability was determined.

For the measurement of tritium incorporation, cells were washed in PBS, three times and incubated with 5 ml of cold thymidine, uridine or leucine appropriately at room temperature for 5 min to remove any non-specific binding. Cells were washed again in PBS, three times and treated with 2 ml of 10% TCA (w/v) for 5 min to remove acid soluble radioactivity. Samples were then digested overnight in 2 ml of 0.5 M NaOH at 37 °C. The radioactivity of samples was determined by scintillation counting.

2.7. Interaction with the telomeric DNA single-strand overhang

Interaction of BRACO-19 with the telomeric overhang was measured using γ-^{32}P-ATP labelled 21C oligonucleotide complementary to the overhang. Aliquots of 2 μg undigested genomic DNA were hybridized with 0.5 pmol of γ-^{32}P-ATP labelled oligonucleotide in potassium buffer overnight at 50 °C. The reaction was stopped by the addition of 6 μl of loading buffer. Samples were separated on 0.8% agarose gel in 1× TBE buffer containing ethidium bromide. Subsequently the gel was dried on Whatman filter paper using a gel drier. Ethidium bromide fluorescence and radioactivity were scanned with a phosphorimager. Results are expressed as relative hybridisation signal normalised to ethidium bromide signal.

2.8. Telomere length analysis

Telomere lengths in cells treated with BRACO-19 were measured using restricted genomic DNA (2 μg) and 0.5 pmol of γ-^{32}P-ATP labelled oligonucleotide as described previously with slight modifications [53]. Genomic DNA was digested overnight with Rsa1 and Hinf1 (1.5 units each) overnight at 37 °C in the presence of γ-^{32}P-ATP labelled oligonucleotide. The reaction was stopped by the addition of 6 μl of loading buffer. Samples were separated on an 0.7% agarose gel containing ethidium bromide in 1× TBE buffer at 115 V for 2 h and 30 min along with a ^{35}S labelled DNA molecular weight marker (Amersham Biosciences). Subsequently the gel was dried on Whatman filter paper using a gel drier and exposed to X-ray film overnight before visualizing with a phosphorimager.

2.9. Electrophoretic mobility gel shift assay (EMSA)

hPOT1 protein was prepared with the TnT Coupled Transcription/Translation system (Promega) using the pET22bPOT1 vector. Oligonucleotides were labelled at the 5′-end with T4 polynucleotide kinase (New England Biolabs) and [γ-^{32}P]ATP (3000 Ci/mmol, Amersham) and gel purified. The binding reactions were performed in 20 μl of the following buffer: 50 mM Tris–HCl (pH 8.0), 100 mM KCl, 2 mM $MgCl_2$, 10% glycerol, 0.1% NP40, 20 nM labelled TEL1 probe in the presence of hPOT1 (2 μg). The SACC1 oligonucleotide (250 nM) and salmon sperm DNA (50 μg/ml) were also added as competitors. BRACO-19 was added at room temperature 15 min before the protein. Then, the protein was added and binding was performed for 15 min at room temperature. Reaction products were separated by electrophoresis in 6% non-denaturing polyacrylamide gels in 0.25× Tris borate EDTA buffer. The gels were run at 180 V for 1.5 h, dried on Whatman DE81 paper at 80 °C and visualized by a Phosphorimager (Typhoon 9210, Amersham).

Oligonucleotides used were as follows: TEL1 5′-TAA-CCCTAACCCTAAGCGAATTCGTCATGCGAATTCGCTTAGGGTT-AGGGTTAGGGTTAGGGTTAGGGTTAGGGTTAGGG-3′ SACC1 5′-ACTGTCGTACTTGATATGTGGGTGTGTGTGGG-3′.

2.10. Immunofluorescence

For immunofluorescence microscopy, HT1080-GFPPOT1 cells plated on glass cover slips were permeabilized in 0.5% Triton X-100/PBS and fixed with 3% paraformaldehyde. Cells were then washed twice in PBS and treated with permeabilization buffer (20 mM Tris–HCl (pH 8.0), 50 mM NaCl, 3 mM $MgCl_2$,

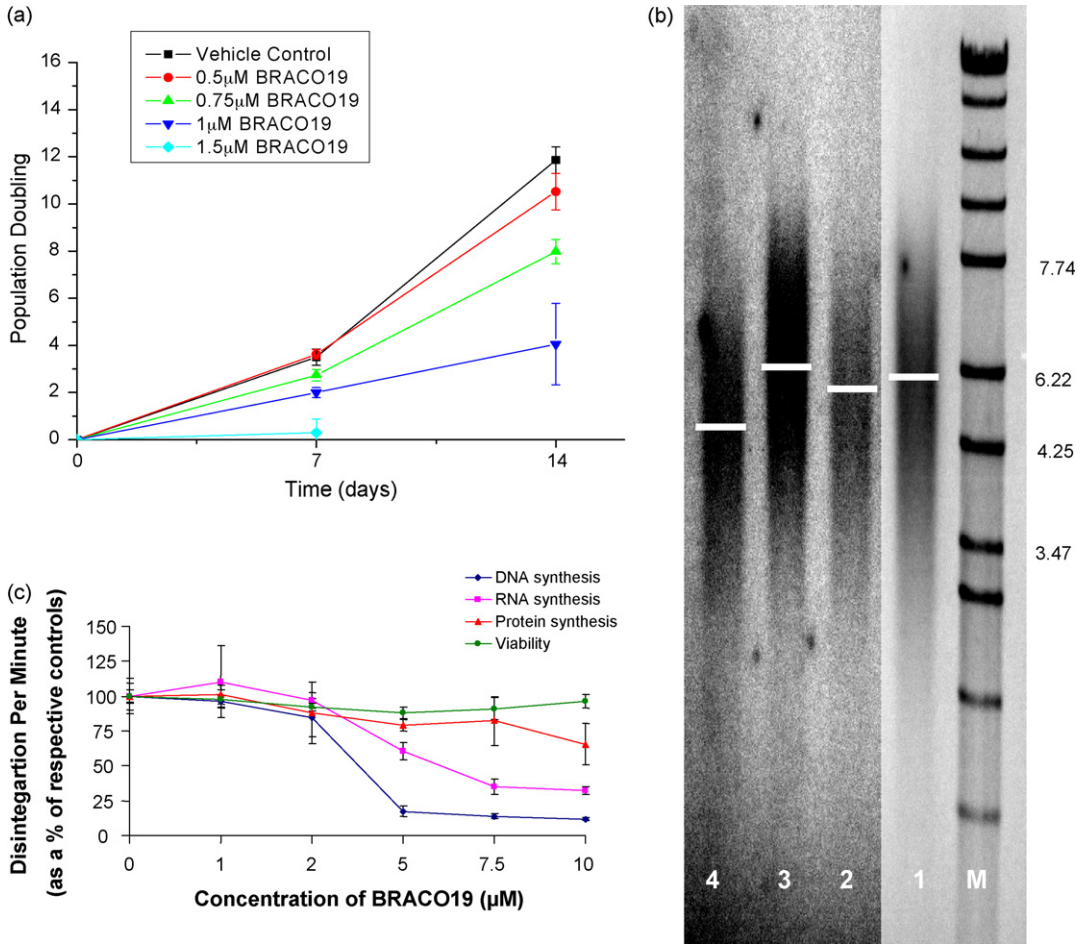

Fig. 2 – (a) Long-term growth inhibition of MCF7 cells exposed to various concentrations of BRACO-19 for 2 weeks in culture. Results are average population doublings of three experiments ± S.E.M. (b) Telomere restriction fragments of A2780 cells exposed to 0 and 2 μM BRACO-19 for up to 5 weeks. Lanes 1 and 2 are from untreated cells at week one and week five, respectively; lanes 3 and 4 are from cells treated with 2 μM BRACO-19 at week one and week five, respectively; M represents a DNA molecular weight marker. (c) Effects of various concentrations of BRACO-19 on DNA, RNA and protein syntheses and viability of MCF7 cells treated for 4 h following labelling with tritiated precursors. All data points are calculated as a percentage of untreated cells.

300 mM sucrose and 0.5% Triton X-100), washed twice with PBS followed by antibody staining with 1 ng/μl for TRF2 4A794 mouse monoclonal (Upstate Biotechnology) in 0.5% Triton X-100/PBS. The nuclear DNA was stained with 1 μM of Hoechst. Secondary antibodies raised against mouse were labelled with Alexa 568 (molecular probes).

For experiments on living cells, EcR293GFP-hPOT1 cells were plated on glass cover slips in complete media supplemented with 0.1 μM of Hoechst 33342. GFP and Hoechst fluorescence were recorded on a heated stage (37 °C) and CO_2 chamber of an Axiovert 200 M inverted microscope (Carl Zeiss, Oberkochen, Germany).

3. Results

BRACO-19 showed optimal growth inhibitory activity in long-term culture at sub-cytotoxic concentrations in all cancer cell lines while showing selectivity between cancerous versus the normal fibroblast cell lines IMR90 and WI-38, as revealed by short-term exposure experiments (Table 1). Fig. 2(a) shows a typical series of population growth curves, with progressive decreases in the rate of population doubling until a threshold is reached, at which point growth is inhibited almost from the

Table 1 – Short-term cytotoxicity in terms of growth inhibitory concentrations for BRACO-19 in a panel of cancer and normal fibroblast (IMR90 and WI-38) cell lines

Cell line	Short-term cytotoxicity (μM)
MCF7	2.5
A549	2.4
DU145	2.3
HT-29	2.7
HGC-27	2.6
A2780	2.5
WI-38	10.7
IMR90	>25

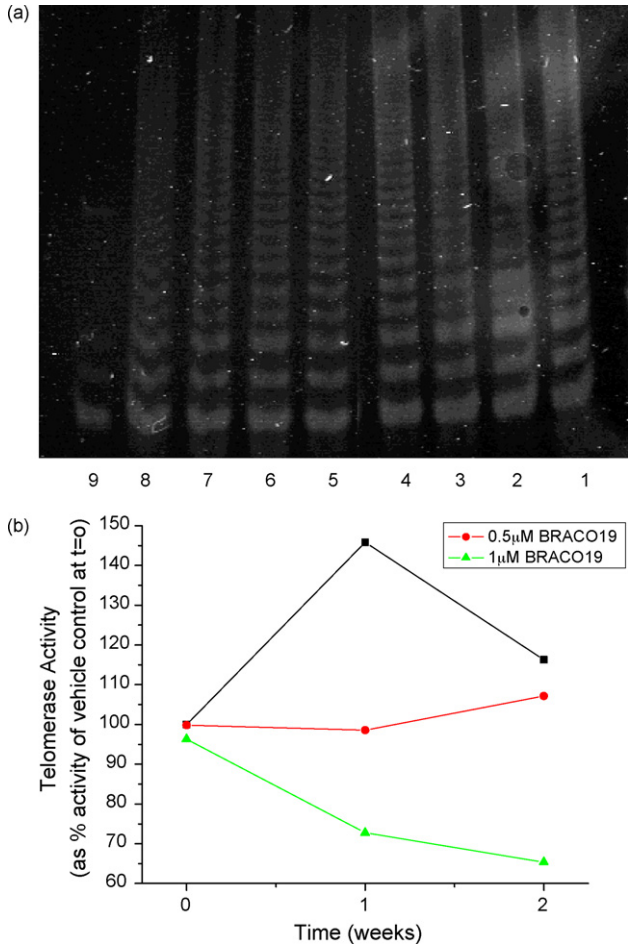

Fig. 3 – Changes in activity of telomerase in MCF7 cells treated with BRACO-19 for a period of 2 weeks, measured using the TRAP assay with 500 ng of telomerase protein extract. (a) The TRAP assay gels. Lanes 1–4 are for vehicle control at weeks 1–4. Lanes 5–8 are for cells administered BRACO-19, and evaluated in the assay at weeks 1–4, respectively. Lane 9 shows a negative control. (b) Enzyme activity is represented as the percentage of untreated sample at time zero, with samples taken immediately after the addition of appropriate concentrations of BRACO-19.

outset of the experiment. Affected cells at this sub-lethal concentration of BRACO-19 (<IC_{50} value) are not killed; instead they are apparently initially quiescent and non-replicating. Telomere shortening, of ca 2 kb, was detected in A2780 cells following a 5-week exposure to BRACO-19 (Fig. 2(b)). This corresponds to an average loss of ca 57 nt per day for this cell line, which has a 24 h doubling time. The small difference in telomere length between treated and untreated cells after 1 week (lanes 1 and 3) is well within the margin of error for telomere length measurements, and we do not consider it to be significant.

Effects on nucleic acid and protein synthesis were evaluated following short-term exposure of MCF7 cells to BRACO-19. Fig. 2(c) shows that changes (notably on DNA and RNA synthesis) were only evident at higher drug concentrations, greater than 2 μM.

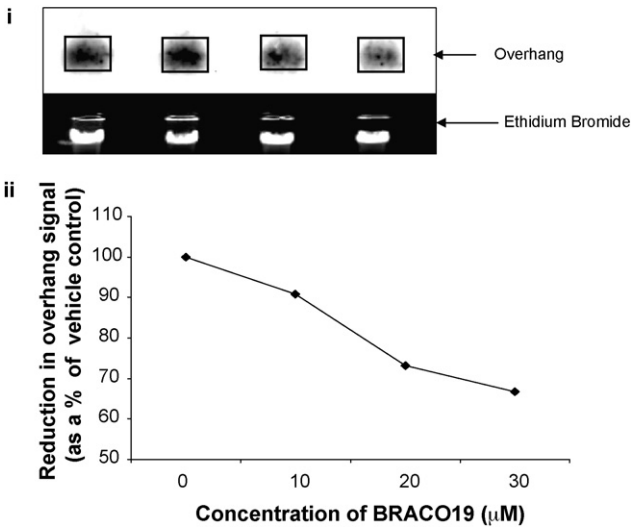

Fig. 4 – Interference of BRACO-19 with the telomeric single-stranded overhang *in vitro*. (i) Overhang signal and corresponding ethidium bromide staining for DNA quantification. (ii) Overhang signal presented as a ratio of overhang signal:DNA, and normalised as a percentage of sample containing BRACO-19.

3.1. *Effects on telomerase and telomeres*

Protein extracts from MCF7 cells treated with BRACO-19 for up to 2 weeks were used to measure telomerase activity using the TRAP assay. This showed that telomerase activity was inhibited by a total of 65% at the end of the 2-week treatment at a 1 μM BRACO-19 concentration compared to the untreated samples (Fig. 3). The inhibition appears to be dose-dependent, so that at the lower 0.5 μM BRACO-19 concentration, there is no significant difference at the end of week two in the level of inhibition compared to untreated samples.

Binding and interference of BRACO-19 at the telomeric single-strand overhang was examined *in vitro* by solution hybridisation studies with ^{32}P-ATP labelled oligonucleotide complementary to the telomeric overhang sequence. DNA extracted from MCF7 cells were incubated overnight with varying concentrations of BRACO-19 and labelled with the oligonucleotide. The data shows a dose-dependent reduction in the overhang signal, indicating that BRACO-19 competes with the oligonucleotide probe and therefore binds to the telomeric overhang (Fig. 4). The maximum reduction in the overhang signal was approximately 35% of the control.

3.2. *Effects on hPOT1 binding*

The effect of BRACO-19 on hPOT1 binding to the TEL1 oligonucleotide, which serves as a reconstituted model for the double-stranded telomere with a short telomeric 3′ overhang, was evaluated by EMSA. Two specific complexes of hPOT1 with the single-stranded extension of TEL1 were detected in the absence of the ligand (Fig. 5(a), see (*) and (**) bands). In the presence of BRACO-19 (2–10 μM), a dose-dependent reduction of the intensity of the signal of the upper complex (*) was observed, while no effect of the ligand

was seen onto the lower complex (**). Quantification indicated that the upper complex (*) is decreased to 45%, in the presence of 10 μM BRACO-19 (Fig. 5(a)ii). These data suggest that the formation of the complex with the lower mobility is preferentially inhibited by the presence of BRACO-19, in agreement with the results obtained for another G-quadruplex ligand, telomestatin [54].

To examine the effect of BRACO-19 on the binding of hPOT1 to telomeres in cultured cells, an immortalized EcR293 cell line expressing GFP-hPOT1 was used. In this cell line, the GFP-hPOT1 has been shown to colocalize with TRF2 and induces telomere length elongation [54]. Microscopic examination of living EcR293GFP-hPOT1 cells treated with BRACO-19 (2 μM) for 48 h indicated a decrease in nuclear GFP-hPOT1 staining in

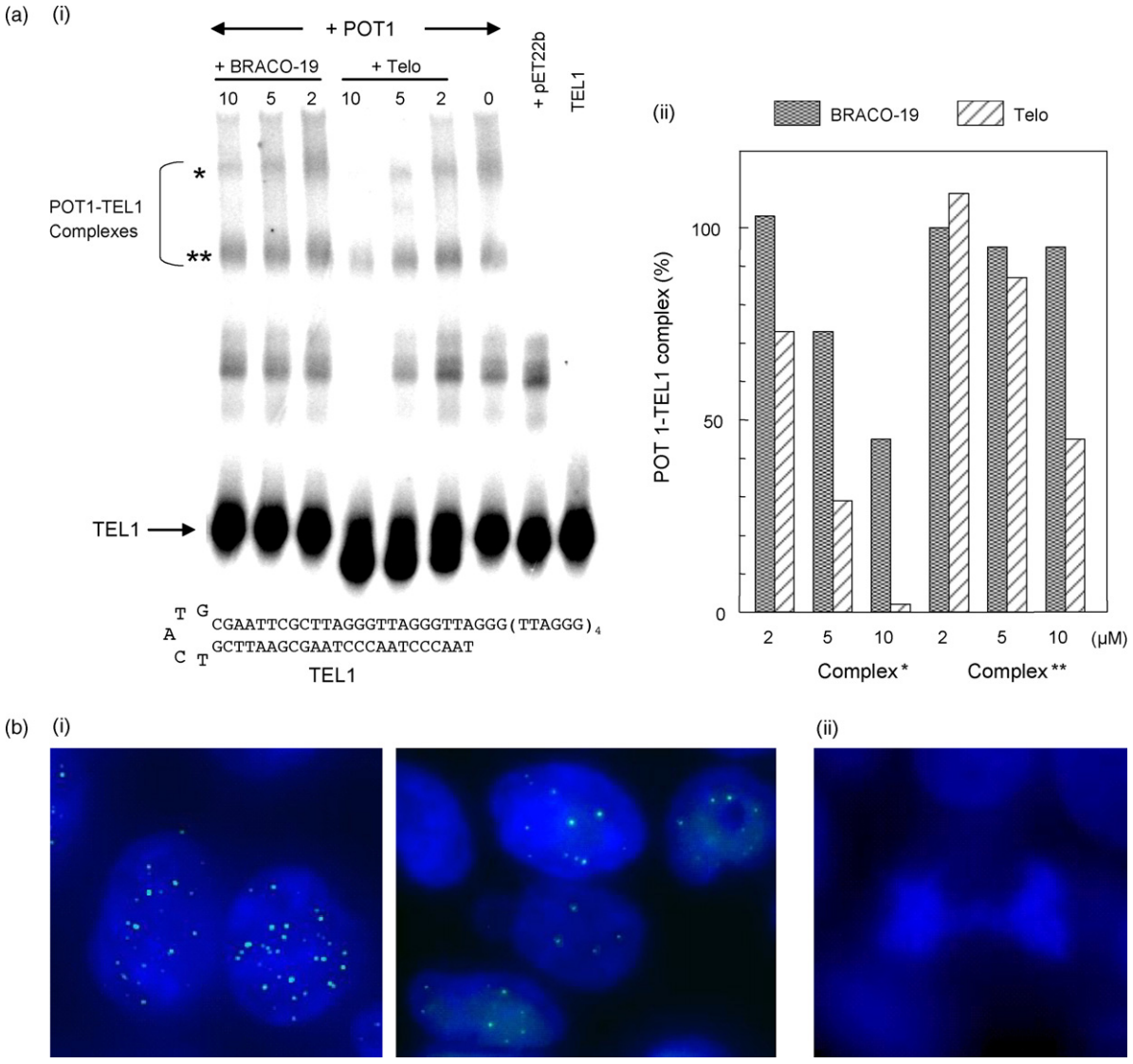

Fig. 5 – The inhibition of POT1 binding to telomeric sequences by BRACO-19. (a): (i) EMSA assay of *in vitro* translated hPOT1 protein (2 μg) on TEL1 oligonucleotide. POT1 forms two specific complexes (*, **) with TEL1 as compared to control vector (+pET22b). The addition of BRACO-19 or telomestatin (2–10 μM) decreases the formation of the POT1/TEL1 complexes. The migration of the free TEL1 probe is indicated by an arrow. (ii) Quantification of the BRACO-19 and telomestatin effect on POT1-TEL1 upper (*) and lower (**) complexes. Results are expressed relative to untreated control. (b) BRACO-19 alters the GFP-POT1 localization at telomeres in EcR293 and HT1080 cells. (i) Effect of BRACO-19 (2 μM) in living EcR293 cells for 48 h on GFP-POT1. Fluorescence for GFP-POT1 (green) and Hoechst (blue) were merged. (ii) A figure showing anaphase bridges induced by BRACO-19 (2 μM, 48 h) in EcR293 cells. (c) Effect of BRACO-19 (10 μM) on GFP-POT1 and TRF2 in HT1080 cells treated for 48 and 72 h. Fluorescence for GFP-POT1 (green), TRF2 (red), Hoechst (blue) and merge were determined on fixed cells. GFP-POT1 colocalizes with TRF2 signal in control HT1080 cells. BRACO-19 treatment induced a marked decrease of the normal telomeric sites of GFP-POT1 fluorescence in an important fraction of the cell population but does not modify TRF2 fluorescence. Some figures of a marked nucleolar accumulation of GFP-POT1 (arrowheads) are also observed in treated HT1080 cells together with the marked GFP-POT1 telomeric decrease. (For interpretation of the references to colour in this figure legend, the reader is referred to the web version of the article.)

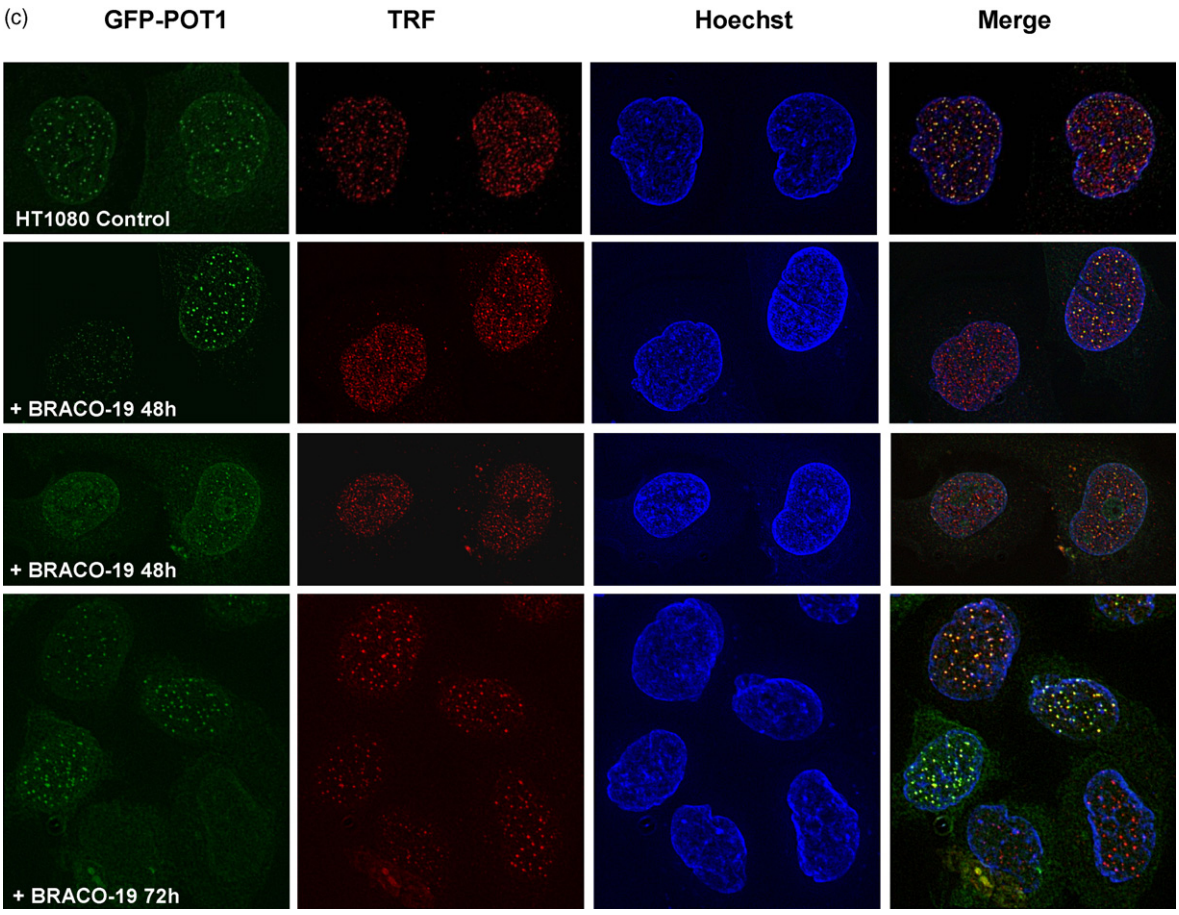

Fig. 5. (Continued).

treated cells (Fig. 5(b)). However, the presence of remaining GFP-hPOT1 telomeric foci suggests that BRACO-19 induces only partial (i.e. incomplete) blocking of GFP-hPOT1 telomeric localization. The presence of anaphase bridges was observed at this ligand concentration, suggesting that the moderate effect to displace GFP-hPOT1 is associated with telomere uncapping activity of BRACO-19 (Fig. 5(b)ii).

These experiments have also been performed using the tumour cell line HT1080 transfected by GFP-hPOT1. We have determined in parallel to the effect on GFP-hPOT1 whether the telomeric localization of TRF2 is also modified by BRACO-19, by using a specific antibody to this protein. We used in these experiments BRACO-19 at 1 and 10 μM, that induces 18 and 55% cell growth inhibition, respectively, for 4 days of treatment. Microscopic examination of treated cells for GFP-hPOT1 and TRF2 fluorescence reveals that BRACO-19 (10 μM for 48 and 72 h) decreases the GFP-hPOT1 signal in a fraction (about 50%) of the treated cell population (Fig. 5(c)) by >50%. Interestingly, the TRF2 signal is not modified in these treated cells, indicating that BRACO-19 does not alter whole telomere integrity. In some of the treated cells, we observed a marked GFP-hPOT1 nucleolar accumulation that parallels the decreased telomeric staining of GFP-hPOT1 (Fig. 5(c)). At this BRACO-19 concentration (10 μM), the presence of anaphase bridges was observed during mitosis, indicating that hPOT1 delocalization is associated with telomere uncapping.

At lower ligand concentration (1 μM), the decrease of the GFP-hPOT1 signal is very faint and is only observed at few telomeric sites, as indicated by the presence of the TRF2 foci without GFP-hPOT1 (result not shown). Altogether these results indicate that BRACO-19 impairs the binding of hPOT1 in a fraction of the HT1080 cell population but does not alter the TRF2 signal.

4. Discussion

We have previously demonstrated that the G-quadruplex stabilising compound, the 3,6,9-trisubstituted acridine BRACO-19, is a potent telomerase inhibitor *in vitro* [47–49], that it produces senescence in several cancer cell lines [50], and that it has *in vivo* anticancer activity both as a single agent [51] and in combination with taxol [52]. We show here that BRACO-19 produces cellular growth arrest in a number of cancer cell lines following long-term exposure at sub-cytotoxic exposure, which is accompanied by a time-dependent decrease in telomerase enzymatic activity. This extends previous observations, which have just been at a single-time-point [47–49], and further supports the concept that inducing the telomeric DNA single-stranded overhang substrate to fold into a G-quadruplex results in telomerase inhibition [18,20]. The observation that the inhibition is only partial, is

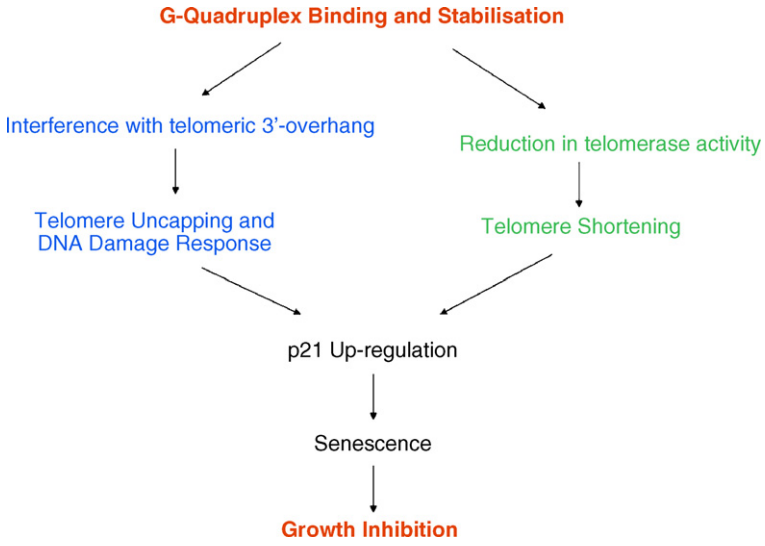

Fig. 6 – Schematic representation of the possible telomere-associated pathways through which BRACO-19 produces cell growth arrest and apoptosis in cancer cells.

consistent with the other findings reported here, that BRACO-19 is ≫100% effective in competing with the hPOT1 protein for the overhang, which serves to disrupt G-quadruplex formation [17]. Telomere length decreases in the A2780 ovarian cancer cell line, after extended exposure, in accord with previous observations of shortening in the UXF1138 vulval carcinoma cell line [51], albeit with an apparently differing rate of telomere loss. These differences in sensitivity against different cell lines may indicate the diversity and the characteristics of the cell lines and their different origins, as well as possible differences in telomere accessibility. We also note that the cellular effects take place at concentrations significantly lower than those required to produce changes in global nucleic acid or protein synthesis, which is strongly suggestive of a non-cytotoxic mechanism of action. In general, potency is lower in the normal fibroblast lines IMR-90 and WI-38 than in the tumour lines, indicative of selective effects in the latter.

Senescence produced by BRACO-19 has been previously shown [50] to be accompanied by up-regulation of *p21*, a molecular marker of senescence, which is apparent after one-week treatment. Similar short-term effects have been noted with a range of G-quadruplex ligands [28,30,45,46] and contrast with the long-term senescence expected only when telomere shortening has reached a critically low point. It may be that a sub-set of the total cell population have critically short telomeres (as suggested by the presence of a short telomere region in the Southern blot gels), and that as a consequence these can rapidly be shortened to the point of senescence onset [55].

It is also feasible that G-quartet formation at the single-stranded overhang uncaps telomerase and hPOT1 from physical association with the 3′-end [54,56], which is known to rapidly induce senescence [57,58] and the induction of a DNA damage response [59–61]. Signals initiated by telomere dysfunction are similar to those initiated due to double-strand DNA breaks, and they are typically mediated by the DNA damage response mediated ATM/ATR-p53–p21 pathway [62]. We suggest that both uncapping and the more classical telomere-shortening are pathways to selective cancer cell apoptosis that are activated by BRACO-19 (Fig. 6). Alterations in telomere capping status have also been suggested to occur in cells treated with the polycyclic acridinium compound RHPS4 [45].

Binding of BRACO-19 to the telomeric 3′ overhang to stabilise quadruplex structures *in vitro* was confirmed by the solution hybridisation of radio-labelled C-rich oligonucleotide complementary to the 3′ single-stranded telomeric DNA overhang. Analogous results have been previously reported for other G-quadruplex ligands such as Telomestatin [62] and the pyridine dicarboxamide compound ^{3}H-360A [63], suggesting that the phenomenon is not restricted to a particular chemical type. BRACO-19 is significantly less potent than telomestatin in this assay, as well as for competition of hPOT1 binding *in vitro* to telomeric sequences [17]. Interestingly, the cellular effect of BRACO-19 in the tumour cell line HT1080GFP-POT1 appears to differ from telomestatin. This ligand produced complete delocalization of POT1 accompanied by a large decrease in the TRF2 signal at double-stranded telomeric sequences [64,65], while BRACO-19 selectively removes the GFP-POT1 signal without any effect on TRF2. Interestingly, the effect of BRACO-19 on GFP-POT1 is related to the formation of anaphase bridges and to the proliferation arrest of the cell population, suggesting a relationship between telomere dysfunction and the antiproliferative effect of the compound. BRACO-19 has been reported [66] to be a 5.8-fold less potent inhibitor of telomerase activity than telomestatin, which concurs with its lower affinity [66] for the human telomeric DNA quadruplex, and which provides an explanation for the findings reported here, of the lower ability of BRACO-19 to disrupt hPOT1-DNA binding in vitro and in vivo. Evidently, though this is still sufficient to result in senescence and selective cancer cell death.

This study has confirmed and extended previous observations [49,50] that BRACO-19 is able to bypass the phenotypic time-lag inherent in a pure telomerase inhibitor, and is

consistent with analogous findings in tumour xenografts [51], that anticancer responses are not associated with any significant time-delays after the onset of treatment. Thus telomere targeting, in conjunction with telomerase inhibition [67], may be a practical and viable new molecular targeting modality for the treatment of human cancer.

Acknowledgements

We are grateful to Cancer Research UK, Antisoma Ltd. and the Ligue Nationale Contre le Cancer (Equipe labellisée 2006) for support of these studies.

REFERENCES

[1] Bryan TM, Cech TR. Telomerase and the maintenance of chromosome ends. Curr Opin Cell Biol 1999;11:318–24.
[2] Kim NW, Piatyszek MA, Prowse KR, Harley CB, West MD, Ho PL, et al. Specific association of human telomerase activity with immortal cells and cancer. Science 1994;266:2011–5.
[3] Shay JW, Wright WE. Telomerase: a target for cancer therapeutics. Cancer Cell 2002;2:257–65.
[4] Greider CW, Blackburn EH. Identification of a specific telomere terminal transferase activity in *Tetrahymena* extracts. Cell 1985;43:405–13.
[5] Autexier C, Lue NF. The structure and function of telomerase reverse transcriptase. Ann Rev Biochem 2006;75:493–517.
[6] Hahn WC, Counter CM, Lundberg AS, Beijersbergen RL, Brooks MW, Weinberg RA. Creation of human tumour cells with defined genetic elements. Nature 1999;400:464–8.
[7] Boehm JS, Hession MT, Bulmer SE, Hahn WC. Transformation of human and murine fibroblasts without viral oncoproteins. Mol Cell Biol 2005;25:6464–74.
[8] Hahn WC, Stewart SA, Brooks MW, York SG, Eaton E, Kurachi A, et al. Inhibition of telomerase limits the growth of human cancer cells. Nat Med 1999;10:1164–70.
[9] Zhang X, Mar V, Zhou W, Harrington L, Robinson MO. Telomere shortening and apoptosis in telomerase-inhibited human tumor cells. Genes Dev 1999;13:2388–99.
[10] Herbert BS, Pitts AE, Baker SI, Hamilton SE, Wright WE, Shay JW, et al. Inhibition of human telomerase in immortal human cells leads to progressive telomere shortening and cell death. Proc Natl Acad Sci USA 1999;96: 14276–81.
[11] El-Daly H, Kull M, Zimmermann S, Pantic M, Waller CF, Martens UM. Selective cytotoxicity and telomere damage in leukemia cells using the telomerase inhibitor BIBR1532. Blood 2005;105:1742–9.
[12] Gellert GC, Dikmen ZG, Wright WE, Gryaznov S, Shay JW. Effects of a novel telomerase inhibitor, GRN163L, in human breast cancer. Breast Cancer Res Treat 2006;96:73–81.
[13] Carpenter EL, Vonderheide RH. Telomerase-based immunotherapy of cancer. Expert Opin Biol Ther 2006;6:1031–9.
[14] Blackburn EH. Switching and signaling at the telomere. Cell 2001;106:661–73.
[15] Wright WE, Tesmer VM, Huffman KE, Levene SD, Shay JW. Normal human chromosomes have long G-rich telomeric overhangs at one end. Genes Dev 1997;11:2801–9.
[16] Sfeir AJ, Chai W, Shay JW, Wright WE. Telomere-end processing: the terminal nucleotides of human chromosomes. Mol Cell 2005;18:131–8.
[17] Zaug AJ, Podell ER, Cech TR. Human POT1 disrupts telomeric G-quadruplexes allowing telomerase extension in vitro. Proc Natl Acad Sci USA 2005;102:10864–9.
[18] Zahler AM, Williamson JR, Cech TR, Prescott DM. Inhibition of telomerase by G-quartet DNA structures. Nature 1991;350:718–20.
[19] Oganesian L, Moon IK, Bryan TM, Jarstfer MB. Extension of G-quadruplex DNA by ciliate telomerase. EMBO J 2006;25:1148–59;
Oganesian L, Bryan TM. Physiological relevance of telomeric G-quadruplex formation: a potential drug target. Bioessays 2007;29:155–65.
[20] Sun D, Thompson B, Cathers BE, Salazar M, Kerwin SM, Trent JO, et al. Inhibition of human telomerase by a G-quadruplex-interactive compound. J Med Chem 1997;40:2113–6.
[21] Mergny J-L, Riou J-F, Maillet P, Teulade-Fichou M-P, Gilson E. Natural and pharmacological regulation of telomerase. Nucleic Acids Res 2002;30:839–65.
[22] Rezler EM, Bearss DJ, Hurley LH. Telomeres and telomerases as drug targets. Curr Opin Pharmacol 2002;2:415–23.
[23] Neidle S, Parkinson GN. Telomere maintenance as a target for anticancer drug discovery. Nat Rev Drug Discov 2002;1:383–93.
[24] Kelland LR. Overcoming the immortality of tumour cells by telomere and telomerase based cancer therapeutics–current status and future prospects. Eur J Cancer 2005;41:971–9.
[25] Harrison RJ, Gowan SM, Kelland LR, Neidle S. Human telomerase inhibition by substituted acridine derivatives. Bioorg Med Chem Lett 1999;9:2463–8.
[26] Perry PJ, Reszka AP, Wood AA, Read MA, Gowan SM, Dosanjh HS, et al. Human telomerase inhibition by regioisomeric disubstituted amidoanthracene-9,10-diones. J Med Chem 1998;41:4873–84.
[27] Mergny J-L, Lacroix L, Teulade-Fichou MP, Hounsou C, Guittat L, Hoarau M, et al. Telomerase inhibitors based on quadruplex ligands selected by a fluorescence assay. Proc Natl Acad Sci USA 2001;98:3062–7.
[28] Riou J-F, Guittat L, Mailliet P, Laoui A, Renou E, Petitgenet O, et al. Cell senescence and telomere shortening induced by a new series of specific G-quadruplex DNA ligands. Proc Natl Acad Sci USA 2002;99:2672–7.
[29] Guittat L, De Cian A, Rosu F, Gabelica V, De Pauw E, Delfourne E, et al. Ascididemin and meridine stabilise G-quadruplexes and inhibit telomerase in vitro. Biochim Biophys Acta 2005;1724:375–84.
[30] Pennarun G, Granotier C, Gauthier LR, Gomez D, Hoffschir F, Mandine E, et al. Apoptosis related to telomere instability and cell cycle alterations in human glioma cells treated by new highly selective G-quadruplex ligands. Oncogene 2005;24:2917–28.
[31] Heald RA, Modi C, Cookson JC, Hutchinson I, Laughton CA, Gowan SM, et al. Antitumor polycyclic acridines. 8. (1) Synthesis and telomerase-inhibitory activity of methylated pentacyclic acridinium salts. J Med Chem 2002;45:590–7.
[32] Cookson JC, Heald RA, Stevens MF. Antitumor polycyclic acridines. 17. Synthesis and pharmaceutical profiles of pentacyclic acridinium salts designed to destabilize telomeric integrity. J Med Chem 2005;48:7198–207.
[33] Shi DF, Wheelhouse RT, Sun D, Hurley LH. Quadruplex-interactive agents as telomerase inhibitors: synthesis of porphyrins and structure-activity relationship for the inhibition of telomerase. J Med Chem 2001;44:4509–23.
[34] Kim M-Y, Vankayalapati H, Shin-ya K, Wierzba K, Hurley LH. Telomestatin, a potent telomerase inhibitor that interacts quite specifically with the human telomeric

intramolecular G-quadruplex. J Am Chem Soc 2002;124:2098–9.
[35] Zhou JL, Lu YJ, Ou TM, Zhou JM, Huang ZS, Zhu XF, et al. Synthesis and evaluation of quindoline derivatives as G-quadruplex inducing and stabilizing ligands and potential inhibitors of telomerase. J Med Chem 2005;48:7315–21.
[36] Guyen B, Schultes CM, Hazel P, Mann J, Neidle S. Synthesis and evaluation of analogues of 10H-indolo[3,2-*b*]quinoline as G-quadruplex stabilising ligands and potential inhibitors of the enzyme telomerase. Org Biomol Chem 2004;2:981–8.
[37] Rossetti L, Franceschin M, Schirripa S, Bianco A, Ortaggi G, Savino M. Selective interactions of perylene derivatives having different side chains with inter- and intramolecular G-quadruplex DNA structures. A correlation with telomerase inhibition. Bioorg Med Chem Lett 2005;15: 413–20.
[38] Franceschin M, Rossetti L, D'Ambrosio A, Schirripa S, Bianco A, Ortaggi G, et al. Natural and synthetic G-quadruplex interactive berberine derivatives. Bioorg Med Chem Lett 2006;16:1707–11.
[39] Izbicka E, Nishioka D, Marcell V, Raymond E, Davidson KK, Lawrence RA, et al. Telomere-interactive agents affect proliferation rates and induce chromosomal destabilization in sea urchin embryos. Anticancer Drug Des 1999;14:355–65.
[40] Grand LC, Han H, Munoz RM, Weitman S, Von Hoff DD, Hurley LH, et al. The cationic porphyrin TMPyP4 down-regulates *c-myc* and human telomerase reverse transcriptase expression and inhibits tumor growth *in vivo*. Mol Cancer Ther 2002;1:566–73.
[41] Tauchi T, Shin-Ya K, Sashida G, Sumi M, Nakajima A, Shimamoto T, et al. Activity of a novel G-quadruplex-interactive telomerase inhibitor, telomestatin (SOT-095), against human leukemia cells: involvement of ATM-dependent DNA damage response pathways. Oncogene 2003;22:5338–47.
[42] Shammas MA, Shmookler Reis RJ, Akiyama M, Koley H, Chauhan D, Hideshima T, et al. Telomerase inhibition and cell growth arrest by G-quadruplex interactive agent in multiple myeloma. Mol Cancer Ther 2003;2:825–33.
[43] Shammas MA, Reis RJ, Li C, Li C, Koley H, Hurley LH, et al. Telomerase inhibition and cell growth arrest after telomestatin treatment in multiple myeloma. Clin Cancer Res 2004;10:770–6.
[44] Shammas MA, Koley H, Beer DG, Li C, Goyal RK, Munshi NC. Growth arrest, apoptosis, and telomere shortening of Barrett's-associated adenocarcinoma cells by a telomerase inhibitor. Gastroenterology 2004;126:1337–46.
[45] Leonetti C, Amodei S, D'Angelo C, Rizzo A, Benassi B, Antonelli A, et al. Biological activity of the G-quadruplex ligand RHPS4 (3,11-difluoro-6,8,13-trimethyl-8H-quino[4,3,2-*kl*]acridinium methosulfate) is associated with telomere capping alteration. Mol Pharmacol 2004;66: 1138–46;
Phatak P, Cookson JC, Dai F, Smith V, Gartenhaus RB, Stevens MF, et al. Telomere uncapping by the G-quadruplex ligand RHPS4 inhibits clonogenic tumour cell growth in vitro and in vivo consistent with a cancer stem cell targeting mechanism. Br J Cancer 2007;96:1223–33.
[46] Cookson JC, Dai F, Smith V, Heald RA, Laughton CA, Stevens MFG, et al. Pharmacodynamics of the G-quadruplex-stabilizing telomerase inhibitor 3,11-difluoro-6,8,13-trimethyl-8H-quino[4,3,2-*kl*]acridinium methosulfate (RHPS4) in vitro: activity in human tumor cells correlates with telomere length and can be enhanced, or antagonized, with cytotoxic agents. Mol Pharmacol 2005;68:1551–8.
[47] Read MA, Harrison RJ, Romagnoli B, Tanious FA, Gowan SH, Reszka AP, et al. Structure-based design of selective and potent G quadruplex-mediated telomerase inhibitors. Proc Natl Acad Sci USA 2001;98:4844–9.
[48] Harrison RJ, Cuesta J, Chessari G, Read MA, Basra SK, Reszka AP, et al. Trisubstituted acridine derivatives as potent and selective telomerase inhibitors. J Med Chem 2003;46:4463–76.
[49] Moore MJ, Schultes CM, Cuesta J, Read MA, Basra SK, Reszka AP, et al. Trisubstituted acridines as G-quadruplex telomere targeting agents. Effects of extensions of the 3, 6- and 9-side chains on quadruplex binding, telomerase activity, and cell proliferation. J Med Chem 2006;49:582–99.
[50] Incles CM, Schultes CM, Kempski H, Koehler H, Kelland LR, Neidle S. A G-quadruplex telomere targeting agent produces p16-associated senescence and chromosomal fusions in human prostate cancer cells. Mol Cancer Ther 2004;3:1201–6.
[51] Burger AM, Dai F, Schultes CM, Reszka AP, Moore MJ, Double JA, et al. The G-quadruplex-interactive molecule BRACO-19 inhibits tumor growth, consistent with telomere targeting and interference with telomerase function. Cancer Res 2005;65:1489–96.
[52] Gowan SM, Harrison JR, Patterson L, Valenti M, Read M, Neidle S, et al. A G-quadruplex-interactive potent small-molecule inhibitor of telomerase exhibiting in vitro and in vivo antitumor activity. Mol Pharmacol 2002;61:1154–62.
[53] Gomez D, Aouali N, Londono-Vallejo A, Lacroix L, Megnin-Chanet F, Lemarteleur T, et al. Resistance to the short term antiproliferative activity of the G-quadruplex ligand 12459 is associated with telomerase overexpression and telomere capping alteration. J Biol Chem 2003;278:50554–62.
[54] Gomez D, O'Donohue M-F, Wenner T, Douarre C, Macadré J, Koebel P, et al. The G-quadruplex ligand telomestatin inhibits POT1 binding to telomeric sequences *in vitro* and induces GFP-POT1 dissociation from telomeres in human cells. Cancer Res 2006;66:6908–12.
[55] Hemann MT, Strong MA, Hao LY, Greider CW. The shortest telomere, not average telomere length, is critical for cell viability and chromosome stability. Cell 2001;107:67–77.
[56] Smith CD, Blackburn EH. Uncapping and deregulation of telomeres lead to detrimental cellular consequences in yeast. J Cell Biol 1999;145:203–14.
[57] Li GZ, Eller MS, Firoozabadi R, Gilchrest BA. Evidence that exposure of the telomere 3′ overhang sequence induces senescence. Proc Natl Acad Sci USA 2003;100:527–31.
[58] Pang TL, Wang CY, Hsu CL, Chen MY, Lin JJ. Exposure of single-stranded telomeric DNA causes G2/M cell cycle arrest in Saccharomyces cerevisiae. J Biol Chem 2003;278:9318–21.
[59] Takai H, Smogorzewska A, de Lange T. DNA damage foci at dysfunctional telomeres. Curr Biol 2003;13:1549–56.
[60] d'Adda di Fagagna F, Reaper PM, Clay-Farrace L, Fiegler H, Carr P, Von Zglinicki T, et al. A DNA damage checkpoint response in telomere-initiated senescence. Nature 2003;426:194–8.
[61] Nur-E-Kamal A, Li TK, Zhang A, Qi H, Hars ES, Liu LF. Single-stranded DNA induces ataxia telangiectasia mutant (ATM)/p53-dependent DNA damage and apoptotic signals. J Biol Chem 2003;278:12475–81.
[62] Gomez D, Paterski R, Lemarteleur T, Shin-Ya K, Mergny J-L, Riou J-F. Interaction of telomestatin with the telomeric single-strand overhang. J Biol Chem 2004;279:41487–94.
[63] Granotier C, Pennarun G, Riou L, Hoffschir F, Gauthier LR, De Cian A, et al. Preferential binding of a G-quadruplex ligand to human chromosome ends. Nucleic Acids Res 2005;33:4182–90.
[64] Tahara H, Shin-Ya K, Seimiya H, Yamada H, Tsuruo T, Ide T. G-Quadruplex stabilization by telomestatin induces TRF2 protein dissociation from telomeres and anaphase bridge

formation accompanied by loss of the 3′ telomeric overhang in cancer cells. Oncogene 2006;25:1955–66.
[65] Gomez D, Wenner T, Brassart B, Douarre C, O'Donohue MF, El Khoury V, et al. Telomestatin-induced telomere uncapping is modulated by POT1 through G-overhang extension in HT1080 human tumor cells. J Biol Chem 2006;281:38721–9.
[66] Lemarteleur T, Gomez D, Paterski R, Mandine E, Mailliet P, Riou J-F. Stabilization of the c-myc gene promoter quadruplex by specific ligands' inhibitors of telomerase. Biochem Biophys Res Commun 2004;323:802–8.
[67] Mo Y, Gan Y, Song S, Johnston J, Xiao X, Wientjes MG, et al. Simultaneous targeting of telomeres and telomerase as a cancer therapeutic approach. Cancer Res 2003;63:579–85.